Communications

Check for updates

ESR spectroscopy

¹⁷O Hyperfine Spectroscopy Reveals Hydration Structure of Nitroxide Radicals in Aqueous Solutions

Fabian Hecker,* Lisa Fries, Markus Hiller, Mario Chiesa, and Marina Bennati*

Abstract: The hydration structure of nitroxide radicals in aqueous solutions is elucidated by advanced ¹⁷O hyperfine (hf) spectroscopy with support of quantum chemical calculations and MD simulations. A piperidine and a pyrrolidine-based nitroxide radical are compared and show clear differences in the preferred directionality of H-bond formation. We demonstrate that these scenarios are best represented in ¹⁷O hf spectra, where in-plane coordination over σ-type H-bonding leads to little spin density transfer on the water oxygen and small hf couplings, whereas π-type perpendicular coordination generates much larger hf couplings. Quantitative analysis of the spectra based on MD simulations and DFT predicted hf parameters is consistent with a distribution of close solvating water molecules, in which directionality is influenced by subtle steric effects of the ring and the methyl group substituents.

Nitroxide radicals play a key role in a variety of studies in chemistry, physics and biology. They are unique spin probes for magnetic resonance and structural biology,[1] spin polarizing agents in dynamic nuclear polarization (DNP)[2] and hydration probes,[3] catalysts in oxidation[4] or polymerization reactions[5] as well as catholytes in organic batteries.[6] Piperidine nitroxides such as 4-hydroxy-2,2,6,6-tetramethylpiperidin-1-oxyl (TEMPOL/T_6) and pyrroline nitroxides such as 3-hydroxymethyl-(1-oxy-2,2,5,5-tetramethylpyrroline (TEMPYL/T_5) are among the best representatives of this class (Figure 1, A/B).[7] For instance, the former are utilized in DNP[8] whereas the latter contain the five-membered ring unit of the widespread methanethiosulfonate spin labels
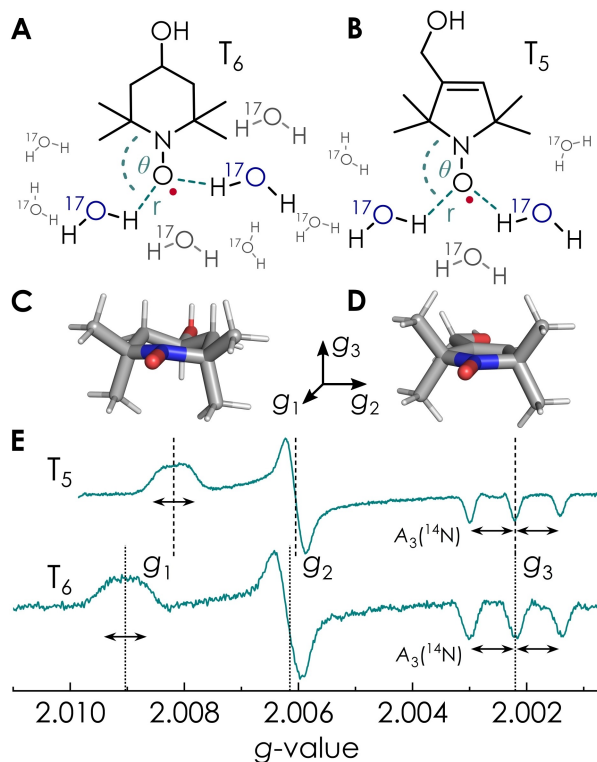

Figure 1. Schematics of nitroxide radicals T_6 (A) and T_5 (B) in bulk ¹⁷O-labeled water with molecules at dihedral angles $\theta(C-N-O_T\cdots H_{wat})$ and distances $r(O_T\cdots H_{wat})$. C/D: DFT optimized structures with g-tensor orientation. E: Echo-detected EPR spectra in ¹⁷O-enriched H_2O of T_6 (bottom) and T_5 (top) recorded at 263 GHz/9.4 T. EPR g-values and A_3 parameters are marked (see text).

[*] Dr. F. Hecker, L. Fries, Dr. M. Hiller, Prof. Dr. M. Bennati
Research Group EPR spectroscopy, Max Planck Institute for Multi-disciplinary Sciences
Am Fassberg 11, 37077 Göttingen (Germany)
E-mail: fabian.hecker@mpinat.mpg.de
marina.bennati@mpinat.mpg.de

L. Fries
Current address: Center for Biostructural Imaging of Neurodegeneration, Medical Center Göttingen
Von-Siebold-Straße 3a, 37075 Göttingen (Germany)
and
NMR Signal Enhancement Group, Max Planck Institute for Multidisciplinary Sciences
Am Fassberg 11, 37077 Göttingen (Germany)

Dr. M. Hiller
Current address: Isotope Technologies Dresden
Rossendorfer Ring 42, 01328 Dresden (Germany)

Prof. Dr. M. Chiesa
Department of Chemistry, University of Torino
Via Giuria 9, 10125 Torino (Italy)

Prof. Dr. M. Bennati
Department of Chemistry, Georg August University Göttingen
Tammanstrasse 2, 37077 Göttingen (Germany)

(MTSL; 1-oxyl-2,2,5,5-tetramethylpyrroline-3-methyl) used in structural biology investigations.[9] The chemical and magnetic resonance properties of nitroxides report on polarity and proticity of their microenvironment, water in particular.[10] Therefore, they have been proposed as valuable probes to detect water in proteins,[11] membranes,[12] and on material surfaces.[13] Moreover, the importance of water in chemical and biological transformations, beyond its role as solvent, has been increasingly recognized[14] and methods for detecting structured water, water clusters and hydration are gaining substantial attention.[15] Electron paramagnetic resonance (EPR) spectroscopy has been extensively used to investigate the environment of nitroxides.[1b] Particularly, the electronic g-values and the hf interaction to the ^{14}N nucleus vary with the polarity around the NO moiety (Figure 1, E).[10,16] Power saturation or saturation recovery experiments[16b,17] as well as Overhauser DNP relaxometry[3,13] provide additional information about hydration structure. However, all these methods rely on indirect observation of water and yield little information about coordination details.

Hyperfine (hf) spectroscopy[18] can directly detect nuclear spins associated with water in the vicinity of nitroxides. The common approach has been through the water protons or via proton/deuterium exchange experiments. However, this information is often ambiguous due to the large abundance of exchangeable protons in the microenvironment.[12,19] On the other hand, the ^{17}O nucleus has been used to detect water coordinated to transition metal ions.[20] In a recent study of a nitroxide-labeled protein, the ^{17}O-H$_2$O signal was observed but no distinct ^{17}O hf couplings were reported.[21] Recently, high-field ENDOR spectroscopy enabled us to resolve individual, structured water molecules coordinated to radical intermediates in an active enzyme.[14b] The ^{17}O hf couplings were found to be fingerprints of in-plane water coordinated to the radical. Motivated by these results, we turned our attention to the widely used class of nitroxides to elucidate their hydration structure in aqueous solutions. In this contribution, we show that the T$_6$ and T$_5$ ^{17}O hf spectra are characterized by a distribution of ^{17}O-H$_2$O hf couplings, however with a clear, preferred directionality of H-bonding. Quantum chemical calculations and MD simulation were used to link the spectroscopic features to the details of structural conformations.

Solutions of ≈200 μM T$_6$ and T$_5$ (Figure 1, A/B) in H$_2$^{17}O/glycerol mixtures (4:1, v:v%) were prepared and shock frozen in liquid N$_2$. All experiments were performed at 50 K cryogenic temperatures where electron spin relaxation times are sufficiently long to perform pulsed hf spectroscopy (see SI1 for Experimental Setup). Echo-detected EPR spectra (Figure 1, E, Figure S1, and Figure S2) did not give evidence for broadening due to ^{17}O exchange with the radical. To exploit spectral resolution and sensitivity, we combined three methods, i.e. hyperfine-sublevel correlation (HYSCORE, SI3), electron-double resonance detected NMR (ED-NMR, SI4) and electron-nuclear double resonance (ENDOR, SI5) at two different polarizing magnetic fields. The three methods are complimentary in terms

of sensitivity and resolution for large and small hf couplings as well as quadrupolar couplings.[18]

Figure 2 summarizes representative experiments, while the full set at 34 and 94 GHz is shown in SI3–SI5. ED-NMR and ENDOR at 94 GHz were recorded at the three canonical excitation positions in the EPR line ($B_0 \| g_{1,2,3}$) but only excitation at $B_0 \| g_3$ allowed for a complete separation from ^{14}N resonances (Figure 2). HYSCORE (A/B), ED-NMR (C) and Davies ENDOR (D) experiments of both nitroxides show broad signals spread over a range of ±4 MHz around the ^{17}O Larmor frequency. The HYSCORE spectra reveal distinct ^{17}O nuclear quadrupole coupling ridges (arrows) and successfully separate ^{14}N signal from the ^{17}O resonance (see SI3). The T$_6$ and T$_5$ ED-NMR spectra complement the HYSCORE data by clearly displaying the intensity distribution of hyperfine couplings. They mainly differ in their signal intensity in the center of the spectrum, which appears better resolved for T$_5$ (see also Figure S9). The Davies ENDOR spectra (Figure 2, D and S12/13) show an overall similar line shape as the ED-NMR spectra, though a slightly decreased spectral resolution. Finally, the Mims ENDOR spectra of T$_5$ clearly reveal sharp signals with a splitting of ≈0.7 MHz (Figure 2, E and Figure S15), while the T$_6$ spectra (Figure 2, E and Figure S14) contain only a matrix line at the ^{17}O Larmor frequency and shoulders at the characteristic Mims blind spots (asterisks). The sharp, almost isotropic T$_5$ resonances are reminiscent of our earlier findings in a protein tyrosyl radical, which we could link to an in-plane coordination of H$_2$^{17}O.[14b] Overall, the screening of methods demonstrated that Mims ENDOR is the only technique capable to catch the small ^{17}O couplings in the T$_5$ radical, while the largest (±4 MHz) hf couplings and quadrupolar couplings can be well characterized by the combination of the other hf techniques.

In order to rationalize the observed spectral features and link them to structural information, we calculated the ^{17}O hf coupling parameters on the density functional theory (DFT) level (B3LYP/EPR-II) from structural models generated by molecular dynamics (MD) simulations (AMBER force field) as well as restricted DFT geometry-optimization (B3LYP/def2-TZVP, details in SI6/SI7). The MD runs were adapted to the frozen solution sample preparation conditions by simulated annealing to 50 K internal temperature. Simulations were repeated with 100 distinct starting conditions to gain a representative sampling of water coordination structures (see SI6).

Evaluation of the three closest waters to the NO moiety from each annealed MD structure revealed two sets of molecules for both nitroxides (Figure 3, A/B): waters H-bonded to the oxygen atom with $r(O_T \cdots H_{wat}) \leq 2.3$ Å and non-bonded, distant waters with $r(O_T \cdots H_{wat}) > 2.3$ Å. Importantly, no water molecules were found in contact to the N atom, neither through their oxygen nor their protons, due to steric hindrance by the methyl-groups (Figure 3, E/G and Figure S20/S21). Glycerol was included in the simulations, however the low content (20 vol%) resulted in only three out of one hundred structures with glycerol H-bonded to the radical (Figure S22).
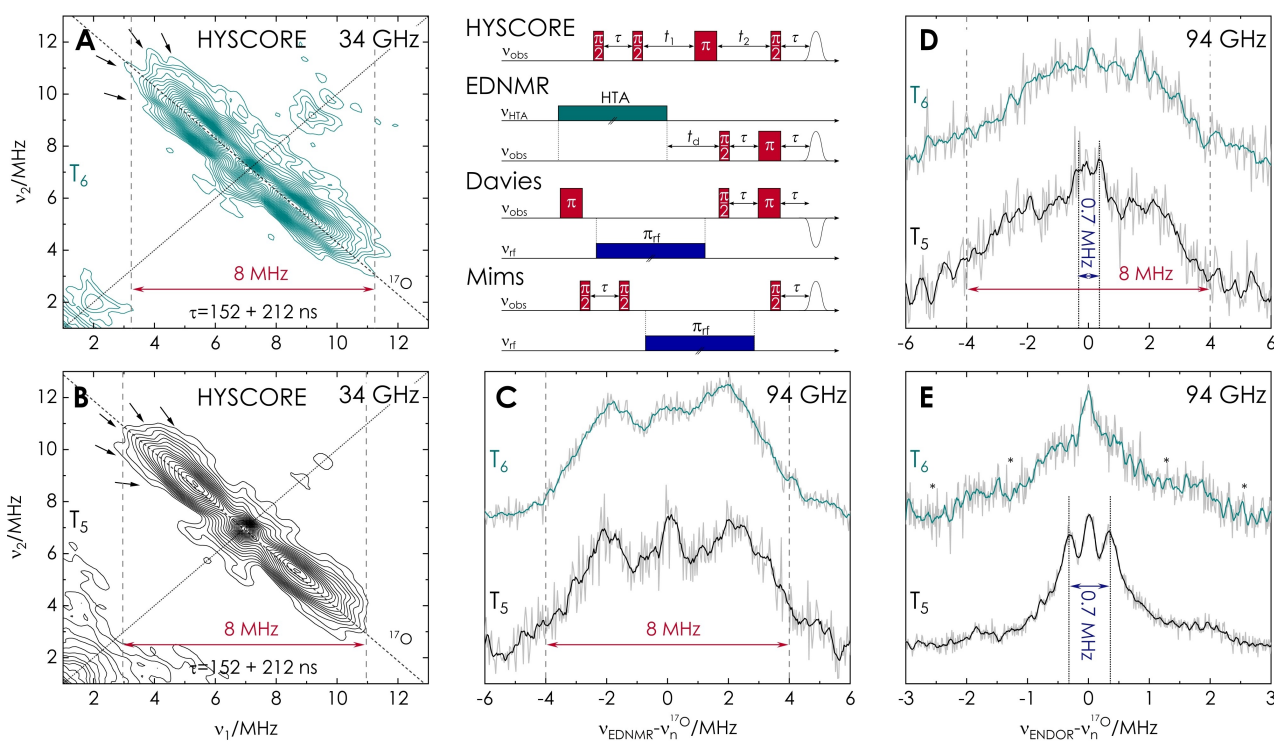
Figure 2. ^{17}O hf spectroscopy experiments of T_6 (cyan) and T_5 (black) and pulse sequences (inset). All experiments shown at $B_0 \parallel g_3$. HYSCORE (A/B) experiments at 34 GHz performed with 6 ns $\pi/2$ pulses. ED-NMR experiments (C) at 94 GHz performed with 30 µs HTA pulses at 0.5 MHz $\omega_{1e}/2\pi$ and selective detection (100/200 ns echo). Davies ENDOR (D) at 94 GHz performed with 400 ns preparation pulses and selective detection. Mims ENDOR (E) at 94 GHz performed with 12 ns $\pi/2$ pulses and $\tau = 390$ ns. Both ENDOR experiments used 30 µs rf pulses. Acquisition times were 12/15 h for HYSCORE, 9 h for ED-NMR, 51/16 h for Davies ENDOR and 6/4 h for Mims ENDOR. Experimental ED-NMR and ENDOR spectra shown in gray with 4th order S.-G. filtered spectra in cyan/black.

The dihedral angle $\theta(C–N–O_T\cdots H_{wat}$, Figure 1) was used to categorize coordination motifs and showed predominantly perpendicular ($\theta = 90/270°$) orientations of H-bonded waters at T_6 (Figure 3, C red) while mostly in-plane ($\theta = 0/180°$) orientations were observed for T_5 (Figure 3, D red). Coordination from the open (or top) face of T_6 ($\theta \approx 90°$) resulted slightly more often than the closed (bottom) face ($\theta \approx 270°$), as expected from the different arrangement of the methyl groups with respect to the two faces (Figure 3, E). The difference in perpendicular vs in-plane coordination is a result of the methyl group arrangement in the chair-like ring of T_6 vs the planar ring of T_5, which in T_6 restricts the access to oxygen lone-pairs as preferred H-bond acceptors (see Figure 3, E/G). The lone-pairs were explicitly treated as pseudo-atoms in the MD simulations following a strategy previously established by Barone et al. (SI6).[22]

We evaluated the individual structures and distinguished between scenarios, in which one versus two waters were in H-bond distance, i.e. $r(O_T\cdots H_{wat}) \leq 2.3$ Å. Structures containing two H-bonds were found overall more populated in T_5 than in T_6 (64 % vs 47 %, respectively, Figure 3, F). Additionally, the in-plane coordination is clearly preferred in T_5 (66 %) versus T_6 (31 %) for structures containing only one H-bonded water.

Energies, g-values, ^{17}O hf and ^{17}O quadrupole couplings were first calculated as a function of different θ values from DFT-geometry optimized small models of a single water H-

bonded to the nitroxides (Figure S7). Energy calculations showed that in-plane and perpendicular water coordination are energetically very closely spaced for both T_6 and T_5, as previously reported for the TEMPO radical (Figure S23).[15] The calculations show that the g_1-values of these nitroxides are slightly affected by the H-bond geometries ($\Delta g_1(90°–0°) \approx 0.0002$, Figure S23). The ^{17}O quadrupole couplings only vary to a small extent with different coordination structures and were therefore considered as constant.[23] The calculated ^{17}O hf couplings, on the other hand, strongly vary with the coordination geometry (Figure 4, A/B, solid lines).

The DFT results in Figure 4, A/B indicate that in-plane coordination leads to small, almost isotropic hf couplings in the range of ≈ 1 MHz because of a small, negative spin density transfer onto ^{17}O through a σ-type H-bonding (Figure 4, C). Instead, perpendicular coordination results in strongly anisotropic hf couplings, with A_3 values up to -10 MHz due to strong interaction in a π-type of H-bonding, with the nitroxides positive spin density, distributed above and below the NO-group (Figure 4, D/E, Figure S24). The negative sign of the hf couplings arises from the negative gyromagnetic ratio γ of the ^{17}O nuclear spin in conjunction with direct spin density transfer via overlap of the NO-SOMO with the H atom of the water. This is opposite to water coordination to transition metal ions where a negative spin density (positive A) is observed due to polarization interactions (bonding via O). Interestingly, a
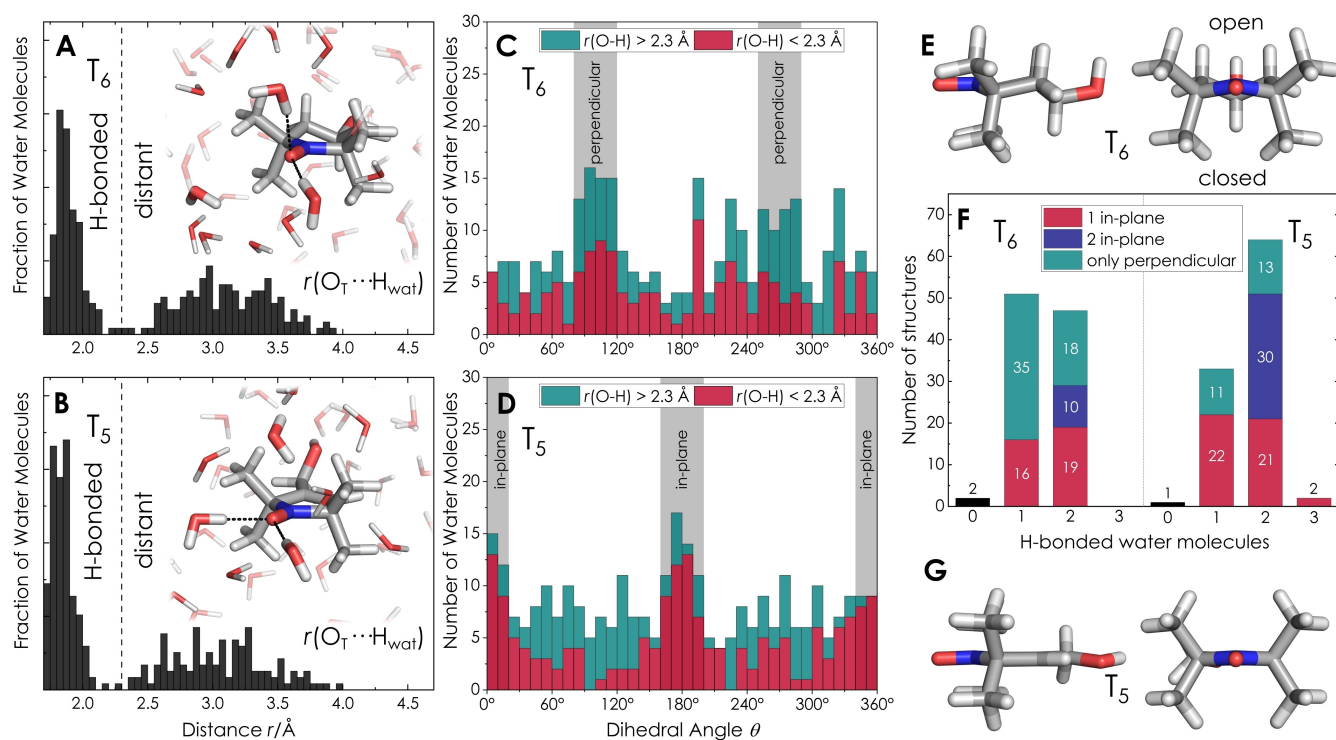
Figure 3. Molecular dynamics analysis of close water coordination to nitroxide radicals. A/B: Distribution of NO oxygen (O_T)–water hydrogen (H_{wat}) distances r from MD, distinguishing between distant ($r(O_T \cdots H_{wat}) > 2.3$ Å) and H-bonded ($r(O_T \cdots H_{wat}) < 2.3$ Å) water molecules. Representative MD structures are shown inset. Three closest water molecules are indicated bold and H-bonds are indicated by dashed lines. C/D: Distribution of dihedral angles θ, showing preferred perpendicular coordination to T_6 (C) and in-plane coordination to T_5 (D) by H-bonded water molecules (red). E/G: DFT-optimized molecular structures of T_6 and T_5 showing the difference in methyl group arrangement that determines access to the oxygen lone pairs as H-bond acceptors. F: Distribution of H-bonded ($r(O_T \cdots H_{wat}) < 2.3$ Å) water molecules found in 100 individual MD structures.

similar ^{17}O hf coupling of 8–10 MHz is observed in water bound perpendicular to $VO(H_2O)_5$ but with opposite sign.[25] Finally we note that coordination from the top (open, 90°) and bottom (closed, 270°) faces of T_6 results in different hf tensors (Figure 4, A, solid lines, Table S3). This arises from the fact that H-bonding from the open face leads to less spin density transfer than from the closed face, (Figure 4 D/E, Figure S24).

In a second step, ^{17}O hf couplings were computed by DFT from the MD structures by considering the 3 closest water molecules (evaluated in Figure 3) plus 3 neighboring waters (or glycerol molecules) to better mimic the bulk sample (SI6). ^{17}O hf coupling of H-bonded waters were plotted as a function of their specific orientation θ (Figure 4, A/B, open circles). In the MD structures, which include-neighboring waters in the second coordination sphere, the difference in hf couplings between the top and bottom coordination of T_6 is lifted (Figure 4, A open circles). For the T_5 radical, the water coordination from top or bottom is almost equally populated (Figure 3, D) and the corresponding couplings result equivalent (Figure 4, B, open circles). The ^{17}O couplings can therefore be used as good indicators of water binding structure.

The broad coupling distribution (up to 8 MHz) in HYSCORE, ED-NMR and Davies ENDOR thus has to arise from perpendicularly coordinated water molecules. No defined features are visible in the spectra, because even

small changes in dihedral angle result in large coupling differences. On the other hand, the sharp doublet with a splitting of ≈ 0.7 MHz in the T_5 Mims ENDOR spectra indicates the presence of in-plane water molecules, as predicted by MD. To verify all these models, we simulated hf spectra as a superposition of the predicted ^{17}O coupling tensors of the H-bonded ($r(O_T \cdots H_{wat}) \leq 2.3$ Å) water molecules from the 100 MD structures (details on simulations with EasySpin[26] in SI1). Figure 5, A/B shows how the MD predicted distribution reproduces the experimental T_6 HYSCORE and Mims ENDOR spectra very well (full set of simulations in Figure S25). The spectra would not be reproduced by individual orientations alone (Figure 5, B, showing for instance the 0° and 90° orientations), underlining the importance of the MD approach. The same simulation approach for the T_5 radical shows that the distribution of strong couplings is underestimated (Figure 5, C and Figure S26). This might be due to a slightly more pronounced accessibility to the radical than predicted in the MD simulations, which contributes to large couplings. In contrast, the distribution in small hf couplings is best reproduced by the MD-based simulations and not compatible with only in-plane (0°/180°) orientations (Figure 5, D). Thus, these results are consistent with distributions of preferred directionalities and are potentially valuable for future benchmarking of DFT and MD calculations.
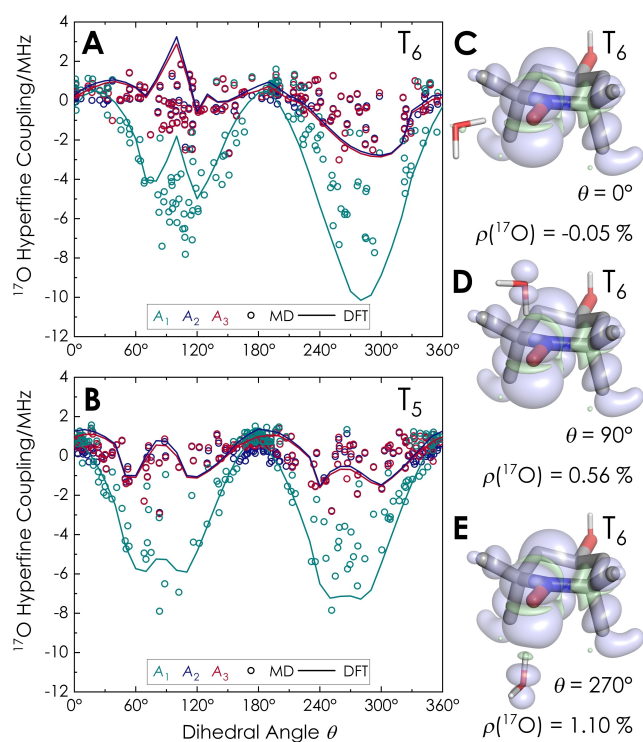
Angew. Chem. Int. Ed. **2023**, e202213700 (4 of 6)

© 2022 The Authors. Angewandte Chemie International Edition published by Wiley-VCH GmbH

Figure 4. A/B: DFT calculated ^{17}O hf couplings (A_1: green, A_2, blue, A_3: red) from DFT geometry-optimized structures of T_6 (A) of T_5 (B) with a single H- bonded water (solid lines, representative tensors in Table S3) and comparison with values from MD structures (open symbols). Uncertainty of DFT is estimated up to 20%. C/D/E: Spin densities from DFT optimized structures of T_6 with one water molecule. Positive (light blue) and negative (light green) spin density shown at the ± 0.0005 a.u. level. Spin density ρ estimated from Loewdin spin population analysis.[24] Spin densities for T_5 are shown in Figure S24.

In summary, we have reported a combination of advanced ^{17}O spectroscopic techniques to detect the hydration structure of nitroxide radicals in frozen aqueous solution. The current resolution of state-of-the-art hf spectroscopy has allowed us to disentangle ^{17}O hf couplings of structured waters that have never been reported before. Particularly 94 GHz Mims ENDOR could capture the differences in the water coordination to the T_5 and T_6 radicals. The differences in solvation of five vs six-membered ring nitroxides are associated to different spin density transfers to waters and should have impact on the electronic properties of the radical. This might be considered in future developments of polarizing agents for DNP experiments in liquids and solids, spin labels to monitor protonation states in biomolecules, or in evaluating the performance of nitroxide-catalyzed reactions. Moreover, we demonstrate the importance of combining spectroscopic techniques with MD simulations and DFT to reproduce distributions of solvating molecules. The results open the opportunity to use nitroxide radicals to probe structured water or solvent molecules in a variety of studies, from structural biology to surface science. Moreover, the protocol can be potentially extended to probe hydration with many organic radicals.
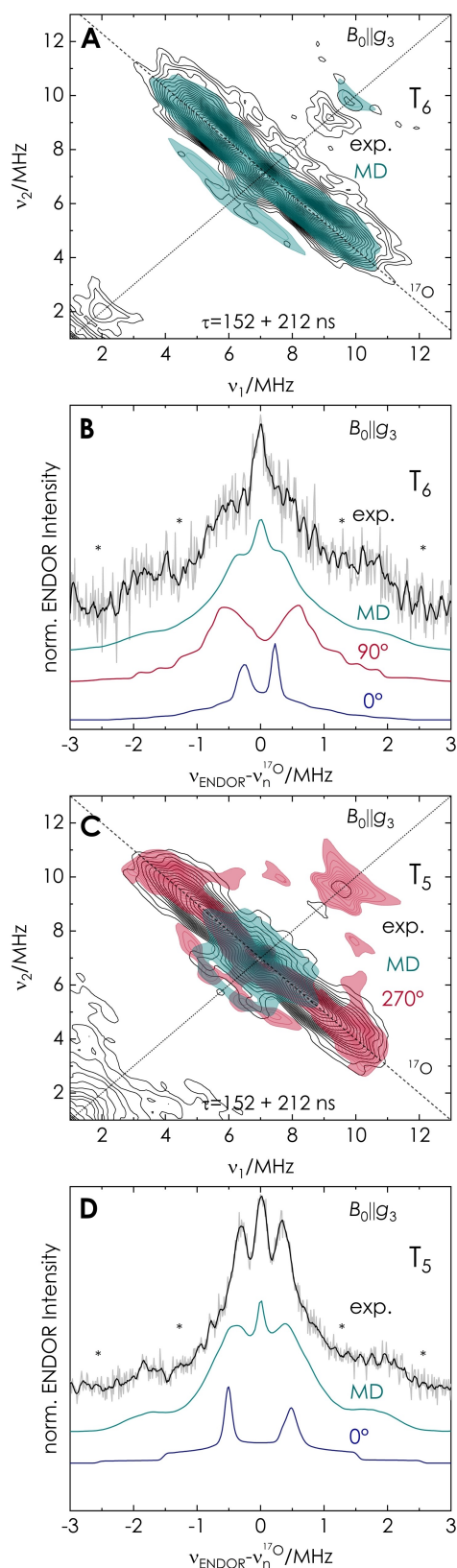

Figure 5. Simulation of ^{17}O HYSCORE (A/C) and Mims ENDOR (B/D) spectra of T_6 (A/B) and T_5 (C/D). Simulations include the sum of 145/167 (T_6/T_5) coupling tensors (Figure 3, F) of H-bonded waters from MD, shown in cyan. Simulations of representative hf coupling tensors for in-plane water (0°) shown in blue and for perpendicular water (90/270°) in red, from Table S3.

Conflict of Interest

The authors declare no conflict of interest.

Data Availability Statement

Original data will be available upon publication from the public Göttingen Research Online database (https://data.goettingen-research-online.de/).

[1] a) N. Kocherginsky, H. M. Swartz, *Nitroxide Spin Labels*, CRC Press, New York, **1995**; b) E. Bordignon, *eMagRes* **2017**, *6*, 235–254.

[2] a) C. Song, K. N. Hu, C. G. Joo, T. M. Swager, R. G. Griffin, *J. Am. Chem. Soc.* **2006**, *128*, 11385–11390; b) G. Liu, M. Levien, N. Karschin, G. Parigi, C. Luchinat, M. Bennati, *Nat. Chem.* **2017**, *9*, 676–680.

[3] J. M. Franck, A. Pavlova, J. A. Scott, S. Han, *Prog. Nucl. Magn. Reson. Spectrosc.* **2013**, *74*, 33–56.

[4] S. Wertz, A. Studer, *Green Chem.* **2013**, *15*, 3116–3134.

[5] B. Keoshkerian, M. K. Georges, D. Boils-Boissier, *Macromolecules* **1995**, *28*, 6381–6382.

[6] H. Fan, B. Hu, H. Li, M. Ravivarma, Y. Feng, J. Song, *Angew. Chem. Int. Ed.* **2022**, *61*, e202115908; *Angew. Chem.* **2022**, *134*, e202115908.

[7] A. Savitsky, A. Nalepa, T. Petrenko, M. Plato, K. Möbius, W. Lubitz, *Appl. Magn. Reson.* **2022**, *53*, 1239–1263.

[8] a) M. Levien, M. Hiller, I. Tkach, M. Bennati, T. Orlando, *J. Phys. Chem. Lett.* **2020**, *11*, 1629–1635; b) G. Stevanato, G. Casano, D. J. Kubicki, Y. Rao, L. Esteban Hofer, G. Menzildjian, H. Karoui, D. Siri, M. Cordova, M. Yulikov, G. Jeschke, M. Lelli, A. Lesage, O. Ouari, L. Emsley, *J. Am. Chem. Soc.* **2020**, *142*, 16587–16599.

[9] a) L. J. Berliner, J. Grunwald, H. O. Hankovszky, K. Hideg, *Anal. Biochem.* **1982**, *119*, 450–455; b) M. F. Peter, C. Gebhardt, R. Machtel, G. G. M. Munoz, J. Glaenzer, A. Narducci, G. H. Thomas, T. Cordes, G. Hagelueken, *Nat. Commun.* **2022**, *13*, 4396.

[10] R. Owenius, M. Engstrom, M. Lindgren, M. Huber, *J. Phys. Chem. A* **2001**, *105*, 10967–10977.

[11] K. Möbius, A. Savitsky, C. Wegener, M. Plato, M. Fuchs, A. Schnegg, A. A. Dubinskii, Y. A. Grishin, I. A. Grigor'ev, M. Kuhn, D. Duche, H. Zimmermann, H. J. Steinhoff, *Magn. Reson. Chem.* **2005**, *43*, S4–S19.

[12] L. Liu, D. J. Mayo, I. D. Sahu, A. Zhou, R. Zhang, R. M. McCarrick, G. A. Lorigan, *Methods Enzymol.* **2015**, *564*, 289–313.

[13] H. Moon, R. P. Collanton, J. I. Monroe, T. M. Casey, M. S. Shell, S. Han, S. L. Scott, *J. Am. Chem. Soc.* **2022**, *144*, 1766–1777.

[14] a) P. Ball, *Proc. Natl. Acad. Sci. USA* **2017**, *114*, 13327–13335; b) F. Hecker, J. Stubbe, M. Bennati, *J. Am. Chem. Soc.* **2021**, *143*, 7237–7241; c) J. Zhong, C. R. Reinhardt, S. Hammes-Schiffer, *J. Am. Chem. Soc.* **2022**, *144*, 7208–7214.

[15] E. M. Brás, T. L. Fischer, M. A. Suhm, *Angew. Chem. Int. Ed.* **2021**, *60*, 19013–19017; *Angew. Chem.* **2021**, *133*, 19161–19165.

[16] a) M. Plato, H. J. Steinhoff, C. Wegener, J. T. Torring, A. Savitsky, K. Mobius, *Mol. Phys.* **2002**, *100*, 3711–3721; b) E. Bordignon, A. I. Nalepa, A. Savitsky, L. Braun, G. Jeschke, *J. Phys. Chem. B* **2015**, *119*, 13797–13806; c) A. Nalepa, K. Möbius, M. Plato, W. Lubitz, A. Savitsky, *Appl. Magn. Reson.* **2019**, *50*, 1–16; d) E. Bordignon, H. Brutlach, L. Urban, K. Hideg, A. Savitsky, A. Schnegg, P. Gast, M. Engelhard, E. J. J. Groenen, K. Möbius, H.-J. Steinhoff, *Appl. Magn. Reson.* **2010**, *37*, 391–403.

[17] C. Altenbach, D. A. Greenhalgh, H. G. Khorana, W. L. Hubbell, *Proc. Natl. Acad. Sci. USA* **1994**, *91*, 1667–1671.

[18] D. Goldfarb, S. Stoll, *EPR Spectroscopy: Fundamentals and Methods*, Wiley, Hoboken, **2018**.

[19] a) A. Volkov, C. Dockter, T. Bund, H. Paulsen, G. Jeschke, *Biophys. J.* **2009**, *96*, 1124–1141; b) L. Urban, H. J. Steinhoff, *Mol. Phys.* **2013**, *111*, 2873–2881.

[20] a) M. Bennati, M. M. Hertel, J. Fritscher, T. F. Prisner, N. Weiden, R. Hofweber, M. Sporner, G. Horn, H. R. Kalbitzer, *Biochemistry* **2006**, *45*, 42–50; b) M. J. Colaneri, J. Vitali, *J. Phys. Chem. A* **2018**, *122*, 6214–6224; c) S. Maurelli, S. Livraghi, M. Chiesa, E. Giamello, S. Van Doorslaer, C. Di Valentin, G. Pacchioni, *Inorg. Chem.* **2011**, *50*, 2385–2394.

[21] A. Nalepa, M. Malferrari, W. Lubitz, G. Venturoli, K. Mobius, A. Savitsky, *Phys. Chem. Chem. Phys.* **2017**, *19*, 28388–28400.

[22] E. Stendardo, A. Pedone, P. Cimino, M. Cristina Menziani, O. Crescenzi, V. Barone, *Phys. Chem. Chem. Phys.* **2010**, *12*, 11697–11709.

[23] D. T. Edmonds, A. Zussman, *Phys. Lett. A* **1972**, *41*, 167–169.

[24] P. O. Löwdin, *J. Chem. Phys.* **1950**, *18*, 365–375.

[25] V. Lagostina, E. Salvadori, M. Chiesa, E. Giamello, *J. Catal.* **2020**, *391*, 397–403.

[26] a) S. Stoll, A. Schweiger, *J. Magn. Reson.* **2006**, *178*, 42–55; b) S. Stoll, R. D. Britt, *Phys. Chem. Chem. Phys.* **2009**, *11*, 6614–6625.
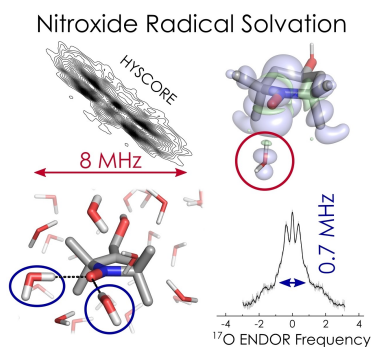
Communications

ESR spectroscopy

F. Hecker,* L. Fries, M. Hiller, M. Chiesa,
M. Bennati* ———————— **e202213700**

[17]O Hyperfine Spectroscopy Reveals Hydration Structure of Nitroxide Radicals in Aqueous Solutions

Nitroxide Radical Solvation

Hydration structure of two different nitroxide radicals in bulk water is investigated by hyperfine spectroscopy that detects $H_2^{17}O$. Combination of ENDOR and HYSCORE methods reveals preferred coordination geometries and H-bonding. Molecular dynamics simulations combined with DFT calculations provided the link between observed spectroscopic parameters and their distribution.